

CHAPTER 3

EXPERIMENTAL METHODS

3.1 Introduction

In this work, poly(ϵ -caprolactone)-based solid and plasticized polymer electrolytes were prepared. The samples were then characterized using experimental techniques such as differential scanning calorimetry, scanning electron microscopy, x-ray diffraction, fourier transform infrared spectroscopy and electrochemical impedance spectroscopy.

3.2 Sample Preparation

The polymer poly(ϵ -caprolactone)(PCL) with $M_n = 80$ kDa as the polymer host and ethylene carbonate (EC) with high purity >99 % as the plasticizer were procured from Sigma Aldrich and used as received. Ammonium thiocyanate (NH_4SCN) purchased from R&M Marketing with $M_w = 76.12$ g mol⁻¹ were dried in an oven at 45 °C for 24 hours prior to use as the dopant salt to supply charge carriers. Tetrahydrofuran (THF) (high purity > 99 %) obtained from J.T. Baker were used as an aprotic solvent.

The PCL-based solid and plasticized polymer electrolytes were prepared by solution casting method with THF as the solvent. The effect of salt concentration and

EC concentration on the properties of the prepared films were determined. Fig. 3.1 depicts how the polymer electrolyte was prepared.

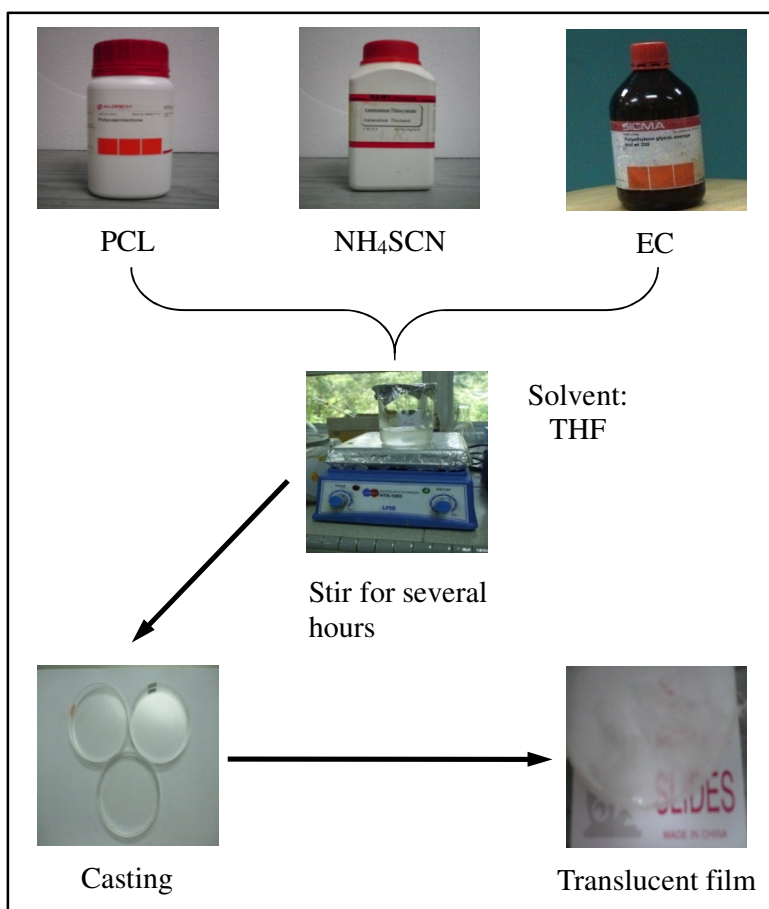


Fig. 3.1 Illustration of polymer electrolyte preparation.

3.2.1 Effect of Salt Concentration on PCL-NH₄SCN Systems

Desired amounts of polymer and salt with various PCL:NH₄SCN ratio in wt.% ranging from 0 to 32 wt.% were dissolved in THF. The mixtures were added together and stirred continuously with a magnetic stirrer for several hours at room temperature to obtain homogeneous solutions. The solutions were then cast into different glass Petri dishes and left to dry at 55 °C for 10 hours. The films were further dried slowly at room

temperature inside a dessicator for two weeks to remove traces of solvent. The present system can form free standing films up to 32 wt.% of salt. Beyond 32 wt.% NH_4SCN , films are no longer mechanically stable. The films used in this study have thickness ranging from 100 to 200 μm .

Table 3.1 lists the weight fraction of the PCL- NH_4SCN prepared samples. The weight of NH_4SCN salt was calculated according to the following equation:

$$W_s = \left(\frac{x}{1-x} \right) W_p \quad (3.1)$$

where W_s is the weight of salt, W_p is the weight of polymer and x is the weight fraction of the salt.

Table 3.1
Weight fraction of the PCL- NH_4SCN samples

x (wt.%)	PCL (g)	NH_4SCN (g)
0	1.0000	0
5	1.0000	0.0526
10	1.0000	0.1111
15	1.0000	0.1765
20	1.0000	0.2500
23	1.0000	0.2987
26	1.0000	0.3514
29	1.0000	0.4085
32	1.0000	0.4706

3.2.2 Effect of EC Concentration on PCL-NH₄SCN-EC Systems

EC was added as plasticizer to the highest conducting sample of PCL-NH₄SCN system. The mixtures of PCL and NH₄SCN were kept at the highest conducting weight ratio and the EC content was varied from 0 to 50 wt.% based on weight of EC divided by total weight of EC and the highest conducting PCL-NH₄SCN complex. All compositions were dissolved in THF and stirred continuously until complete dissolution. The plasticized polymer electrolytes were prepared by the solution cast method as stated in section 3.2.1. The influence of plasticizer concentration on the properties of PCL-NH₄SCN-EC systems was then examined.

Table 3.2 presents the weight fraction of the PCL-NH₄SCN-EC prepared samples. The weight of NH₄SCN salt was calculated according to equation 3.1. The W_s refers to the weight of EC while W_p is the total weight of polymer and salt at the highest conducting ratio from the PCL-NH₄SCN system.

Table 3.2
Weight fraction of the PCL-NH₄SCN-EC samples

x (wt.%)	PCL+ NH ₄ SCN (g)	EC (g)
0	1.3514	0
10	1.3514	0.1502
20	1.3514	0.3379
30	1.3514	0.5792
40	1.3514	0.9009
50	1.3514	1.3514

3.3 Differential Scanning Calorimetry (DSC)

The Differential Scanning Calorimetry (DSC) is a thermal analysis that determines the temperature and heat flow associated with material transitions as a function of temperature and time. Usually the sample and reference pans are in separate furnaces heated by separate heat sources. The difference in heat energy required to maintain both the sample and reference at the same temperature is measured as a function of temperature and time. Heat will flow into or out of the sample as a result of endothermic or exothermic processes, respectively.

There are four basic units of a DSC system. The furnace system is used to heat the sample and reference pans according to a set of temperature program. The automatic sampler unit is programmed to load and unload the pans. A cooling system is necessary to cool the sample and assist in achieving the aimed temperature program. Finally, an interface is set to link between the user and the instrument and enables automatic control of instrument.

DSC can be used to measure a number of thermal properties of a sample such as glass transitions temperature, T_g [Vieira *et al.*, 2008], melting point, T_m , crystallisation temperature, T_c , heat of fusion, ΔH_m [Pan *et al.*, 2007], heat capacity, oxidation stability, degree of cure and reaction kinetics. A schematic diagram of a differential thermogram is illustrated in Fig. 3.2 and the required sample size for the corresponding type of measurement is given in Table 3.3.

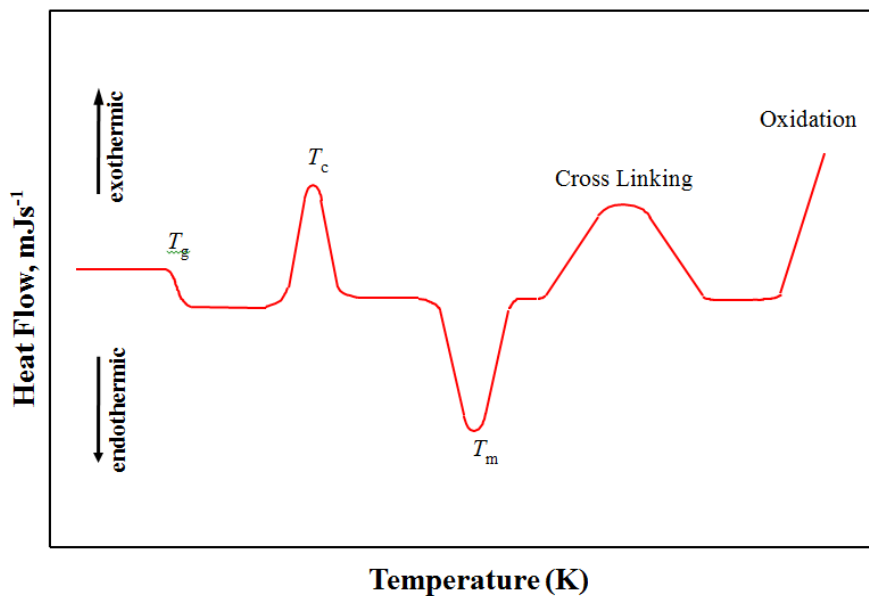


Fig. 3.2 Schematic diagram of a DSC thermogram

Table 3.3
The required sample size of different type of measurement

Type of measurement	Sample size (mg)
Glass transition temperature	10 to 20
Melting point	2 to 10
heat of fusion	5 to 10
heat capacity	10 to 70
oxidative stability	5 to 10
reaction kinetics	5 to 10

Since the thermal history of the sample affects most of the thermal properties, heat-cool-heat experiment was performed to all the samples. The first heat recorded the uncontrolled thermal history data, which would not be used in this work. The second heat data is a function of the sample with known and controlled thermal history and therefore is used to analyze the T_g , T_m and ΔH_m . The relative degree of crystallinity,

χ_c , of the sample can be calculated according to:

$$\chi_c = \frac{\Delta H_m}{\Delta H_m^0} \times 100 \% \quad (3.2)$$

It is noted that some researchers use equation 3.2 to calculate the absolute degree of crystallinity by taking ΔH_m^0 as the melting enthalpy of 100 % crystalline polymer. However, the authentic samples of 100 % crystalline polymer are very rare [Wunderlich, 1990] and literature values very often differ from one another [Guo and Groeninckx, 2001; Honma *et al.*, 2003; Fonseca *et al.*, 2007]. Another way is to take ΔH_m^0 as the melting enthalpy of pure polymer membrane [Kuila *et al.*, 2007] to estimate the relative degree of crystallinity. The present work is using the latter definition where ΔH_m^0 is the melting enthalpy of pure PCL membrane prepared by this work. It means χ_c is the relative value by comparing PCL-salt films to unsalted pure PCL film. A DSC instrument used in this work is presented in Fig. 3.3.



Fig. 3.3 DSC machine: TA Instruments DQ200

3.4 Scanning Electron Microscope (SEM)

The Scanning Electron Microscope (SEM) is an instrument to examine the physical topography and morphology of a sample. A beam of electrons will first be generated by an electron gun. This electron beam will be accelerated by applying high potential between 5 and 50 kV, passes through an electron lens system and finally focuses on the surface of the sample.

For insulating samples, it will build up an electrostatic charge leading to variations of surface potential. Eventually the SEM image could be deteriorated. Therefore, prior to any scan, the samples are vacuumed and coated with a thin layer of conductive material. The conductive layer such as gold coating can also serve to transfer heat (due to electron bombardment) away from the sample during imaging.

SEM can be used to check whether the sample surface is smooth and homogeneous which is an indicator of good miscibility of a polymer blend. If the SEM micrograph shows grainy surface with many new crystals, it may be due to excessive salt in the polymer electrolyte system [Woo *et al.*, 2012]. SEM images may also show new pore-like type morphology, polygon-like spherulites [Choi *et al.*, 2007] and surface morphology changes from soft to brittle [Pereira *et al.*, 2009].

In this work, morphology of the samples was characterized at room temperature using Leica's scanning electron microscope (SEM) model S440 at 10 kV, as shown in Fig. 3.4. All the samples were coated with a thin layer of gold prior to the scanning.



Fig. 3.4 SEM machine: Leica's model S440

3.5 X-ray Diffraction (XRD)

X-rays are electromagnetic radiation with a wavelength about 1 \AA (10^{-10} m) which is comparable to the size of an atom. X-ray diffraction (XRD) has been widely used in two applications, for the fingerprint characterization and structure determination. Each crystalline solid has its own unique XRD pattern which may be used for material identification. Once the material has been identified, its structure can be determined, which makes it an important tool in solid state chemistry and materials science.

XRD is a non-destructive analytical technique. XRD studies have been used to understand the physical properties of metals, polymeric and solid materials. For a semi crystalline material, XRD will capture sharp peaks from the crystalline component and a broad halo like a hump from the amorphous part. The degree of crystallinity can then be

calculated using some application software. Many researchers have used XRD to study the amorphous nature [Awadhia and Agrawal, 2007], crystallite size [Yang *et al.*, 2006] and polymer-salt complexation [Shin *et al.*, 2002; Hirankumar *et al.*, 2005].

In the present work, XRD is employed to study the nature of polymer so that the degree of crystallinity of the polymer membrane can be determined. Fig 3.5 shows the schematic diagram of x-ray diffraction pattern. The regularly arranged molecules in the polymer act as diffraction grating and eventually produce sharp and narrow Bragg peaks. The amorphous region is represented by a less intense broad halo.

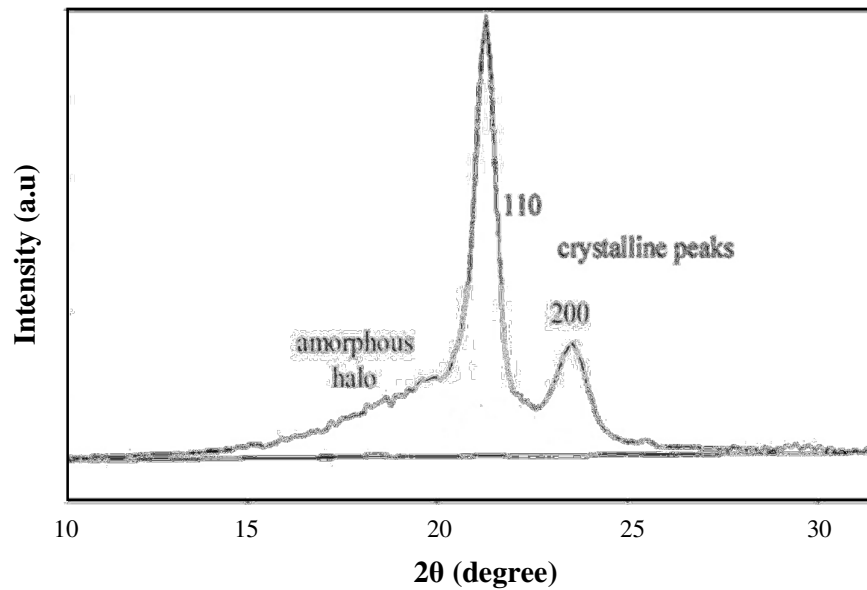


Fig 3.5 Schematic diagram of XRD pattern of polyethylene [Lagaron *et al.*, 2000].

The relative χ_c can be estimated using the simplicity approach of two phase model from XRD result [Hodge *et al.*, 1996] according to equation:

$$\chi_c = \frac{I_c}{(I_c + I_a)} \times 100 \% \quad (3.3)$$

A survey on literature shows that I can be taken as intensity [Pawlicka *et al.*, 2008] (magnitude of y-axis) or integrated area [Wang *et al.*, 2005a] (area under the curve) of the respective peak. This report is using the latter definition where I_c refer to the total crystalline integrated area at Bragg peaks $2\theta = 21.4^\circ$, 22.0° and 23.7° ; I_a is amorphous integrated area of the halo centered on $2\theta = 21.0^\circ$, underneath the crystalline reflections.

In order to decompose overlapping spectrum (separate the crystalline peak from broad halo), all X-ray patterns were deconvoluted with the curve fitting routine in OriginPro 8 software. Baseline correction was done prior to fitting multi-peaks using Gaussian distribution. Linear baselines were used. Eventually, band positions and areas were derived from the curve-fitting routine with high goodness of fit, R^2 within 0.97-0.99.

In this work, XRD measurements were performed using an automated SIEMENS D5000 X-ray diffractometer as presented in Fig. 3.6, equipped with monochromatic Cu-K α radiation (wavelength = 1.5406 Å). This instrument basically requires an X-ray source, a detector to detect the diffracted signals and the samples. The X-ray radiation is usually emitted by copper with a characteristic wavelength $K_\alpha = 1.5406$ Å. When the incident ray strikes a sample, diffraction occurs. The diffracted rays are captured by a moveable detector which is connected to a chart recorder. The counter is usually set to scan over a range of 2θ values from 5 to 80° .



Fig. 3.6 XRD machine: SIEMENS D5000

3.6 Fourier Transform Infrared Spectroscopy (FTIR)

Fourier transform infrared (FTIR) spectroscopy is one of the fast methods to determine the molecular structure on a wide variety of compounds. It is both a qualitative and quantitative analysis. An IR radiation does not have enough energy to induce electronic transitions and is restricted to compounds with small energy differences in the vibrational and rotational states. Each functional group molecule rotates or vibrates at a specific frequency corresponding to some discrete energy levels.

When an infrared radiation reaches a material, some photons are absorbed by the material. Resonance occurs when the radiation energy matches the discrete energy levels of the molecules in the material. The remaining photons pass through the molecules and strike the detector. Then, the detector sends a signal to the computer and

interprets the data. Finally, FTIR captures this vibrational spectrum that displays the unique structural properties of the tested compound. The basic requirement for this infrared activity is that the dipole moment must have a net change during the vibration of the molecules.

In polymer electrolyte systems, the interaction between cations, anions, polymer, and plasticizers could be manifested through FTIR spectra as frequency shifts, changes in band shapes, intensities or splitting of the band. Many researchers have made use of FTIR to investigate polymer electrolyte systems based on PEO [Mitra and Kulkarni, 2002], PAN [Starkey and Frech, 1997] and PMMA [Kumar and Sampath, 2005].

In this work, a comparative study of pure PCL, PCL-NH₄SCN and PCL-NH₄SCN-EC systems will be discussed. The interaction of polymer, salt and plasticizer is expected to occur at the carbonyl function group of PCL and EC located from 1720 to 1736 cm⁻¹ and 1766 to 1784 cm⁻¹, respectively. Thin film used in IR testing were cut into small sizes and placed in the sample holder of the spectrometer.

The IR spectra in this study were recorded using the Thermo Scientific (Nicolet iS10) spectrophotometer as depicted in Fig. 3.7. All the IR spectra were within the wave number range from 650 to 4000 cm⁻¹ operating at a resolution of 1 cm⁻¹. Each spectrum runs 32 scans in 2 s with correction against the background spectrum of air. Dry nitrogen was used for purging purposes in order to exclude the infrared active H₂O and CO₂ in the atmosphere.



Fig. 3.7 FTIR machine: Thermo Scientific Nicolet iS10

3.7 Electrochemical Impedance Spectroscopy (EIS)

The HIOKI 3532 Z LCR Hi-tester as shown in Fig. 3.8 has been used to carry out the impedance measurement in the frequency range from 50 Hz to 5 MHz. The polymer electrolyte films were cut into small discs with a diameter of 2.2 cm and sandwiched between two polished stainless steel blocking electrodes. The diameter of the electrode is 2 cm.

From the impedance plot, an idealized equivalent circuit composed of discrete electrical components can be employed to fit the data. For example, impedance for resistor is R , capacitor is $-j/\omega C$ and inductor is $j\omega L$. Fig. 3.9 presents some complex impedance plots and the corresponding equivalent circuits.

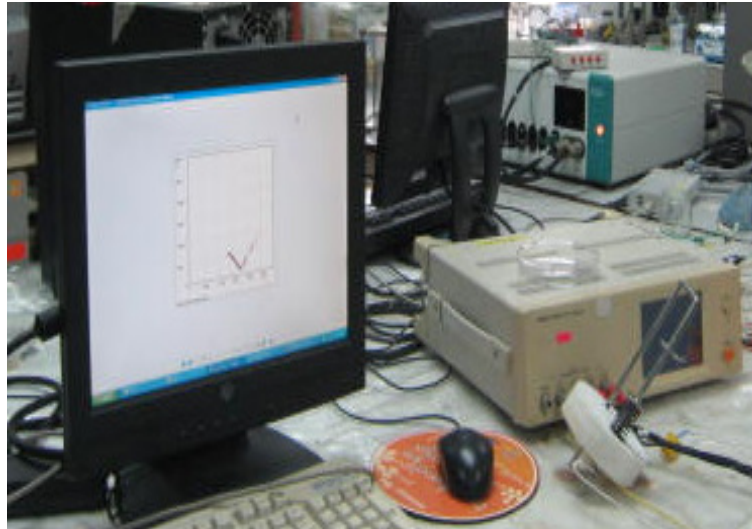


Fig. 3.8 EIS instrument: HIOKI 3532 Z LCR Hi-tester

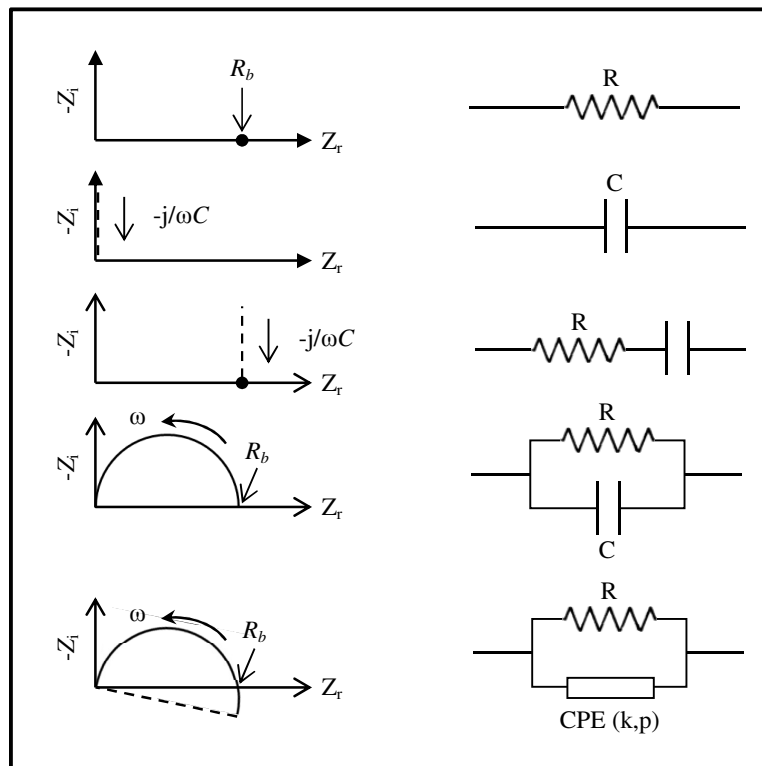


Fig. 3.9 Some impedance plots and the corresponding equivalent circuits.

In polymer electrolyte systems, the impedance plot often shows a depressed semicircle that can be represented by a resistor in parallel connection to an electrical component called a constant phase element (CPE). The impedance of the CPE, Z_{CPE} can be expressed by:

$$Z_{CPE} = k(j\omega)^{-p} \quad (3.4)$$

where k represents a coefficient of constant phase element and p is a dimensionless experimental parameter between zero and unity [MacDonald, 1987]. When $p = 1$, the CPE would become identical to a capacitor C with $k = C^{-1}$ and $Z_C = (j\omega C)^{-1}$. For $p = 0$, the CPE behaves as a resistor with $k = R$ and $Z_R = R$.

3.7.1 Conductivity studies

The electrical conductivity can be calculated using the equation:

$$\sigma = \frac{d}{R_b A} \quad (3.5)$$

where σ is the dc conductivity, d is thickness of the electrolyte film, A is the surface area of contact and R_b is the bulk electrolyte resistance. R_b can be obtained from the impedance plot at the low frequency side of the semicircle intercept on the real impedance axis or at the high frequency side of the spike intercept on the real

impedance axis or the fitting of experimental data using the appropriate equivalent circuit.

3.7.2 Dielectric Behavior

The impedance data can also be transformed to complex relative permittivity, complex electric modulus and loss tangent data to catch a glimpse of ionic conduction mechanism.

The relative permittivity ϵ_r^* is a dimensionless ratio of permittivity, ϵ^* to the permittivity of free space, ϵ_0 . It can also be described in complex form (as a function of angular frequency) that has a real and an imaginary component. These two components are 90° out of phase according to:

$$\epsilon_r^*(\omega) = \frac{\epsilon^*(\omega)}{\epsilon_0} = \epsilon'(\omega) - j\epsilon''(\omega) \quad (3.6)$$

Here $\epsilon_0 = 8.854187817 \times 10^{-12} \text{ F m}^{-1}$, ϵ' and ϵ'' are the real and imaginary part of relative permittivity, respectively, and $j = \sqrt{-1}$. ϵ' and ϵ'' can be calculated from the impedance data according to:

$$\epsilon_r^* = \epsilon' - j\epsilon'' = \frac{1}{j\omega C_0 Z^*} = \frac{Z''}{\omega C_0 (Z'^2 + Z''^2)} - j \frac{Z'}{\omega C_0 (Z'^2 + Z''^2)} \quad (3.7)$$

where Z^* is complex impedance ($Z^* = Z' - jZ''$), C_0 is vacuum capacitance ($C_0 = \epsilon_0 A/d$), d is thickness of the electrolyte film, A is the surface area of contact and ω is angular frequency ($\omega = 2\pi f$).

The electric modulus is defined as the reciprocal of relative permittivity. The relationship between electric modulus, relative permittivity and impedance are given in the following equations:

$$M^* = M' + jM'' = \frac{1}{\epsilon_r^*} = \frac{1}{\epsilon' - j\epsilon''} = \frac{\epsilon'}{\epsilon'^2 + \epsilon''^2} + j \frac{\epsilon''}{\epsilon'^2 + \epsilon''^2} \quad (3.8)$$

$$M^* = j\omega C_0 Z^* = \omega C_0 Z' + j\omega C_0 Z'' \quad (3.9)$$

The conductivity relaxation time for ionic motion can be calculated from the analysis of loss tangent as a function of frequency. The loss tangent, $\tan \delta$ can be obtained from the following ratio:

$$\tan \delta = \frac{\epsilon''}{\epsilon'} = \frac{Z'}{Z''} \quad (3.10)$$

The complex conductivity can also be obtained to check and balance the dc conductivity calculated directly from impedance plot. Complex conductivity can be determined from the following relation:

$$\sigma^* = \sigma' + j\sigma'' = j\omega\epsilon_0\epsilon_r^* = \omega\epsilon_0\epsilon'' + j\omega\epsilon_0\epsilon' \quad (3.11)$$

The real part of complex conductivity can also be analyzed using the Jonscher's universal power law [Murugaraj *et al.*, 2003] as:

$$\sigma' = \sigma_{dc} + A\omega^S \quad (3.12)$$

where σ_{dc} is the dc conductivity, A is the coefficient that depends on temperature and S is the power law exponent in the range between 0 and 1.

3.8 Summary

With these experimental methods, experiments have been carried out on the samples in order to address the objectives stated in Chapter 1.